*International Journal of Minerals, Metallurgy and Materials*
*Volume 20, Number 2, February 2013, Page 146*
**DOI: 10.1007/s12613-013-0706-7**

# Study on stable and meta-stable carbides in a high speed steel for rollers during tempering processes

*Jing Guo*[1)], *Hong-wei Qu*[1)], *Li-gang Liu*[1)], *Yan-liang Sun*[1)], *Yue Zhang*[2)], *and Qing-xiang Yang*[1)]

1) State Key Laboratory of Meta-stable Materials Science and Technology, Yanshan University, Qinhuangdao 066004, China
2) School of Material Science and Engineering, University of Science and Technology Beijing, Beijing 100083, China
(Received: 16 March 2012; revised: 7 May 2012; accepted: 9 May 2012)

**Abstract:**A high speed steel (HSS) was studied for rollers in this work. The steel was quenched at 1150°C and tempered at 520°C. The phase structures of the steel were determined by X-ray diffraction (XRD), and the hardness of specimens was measured. The volume fraction of carbides was counted by Image-Pro Plus software. The typical microstructures were observed by field emission scanning electron microscope (FESEM). Stable and meta-stable carbides were deduced by removing the existing phases one by one in the Fe-C equilibrium calculation. It is found that the precipitated carbides are bulk-like MC, long stripe-like $M_2C$, fishbone-like $M_6C$, and daisy-like $M_7C_3$ during the tempering process. The stable carbides are MC and $M_6C$, but the meta-stable ones are $M_2C$, $M_7C_3$, and $M_3C$.

**Keywords:** high speed steel; phase diagrams; tempering; carbides

## 1. Introduction

With the rapid development of the steel industry and the continuous improvement of rolling technology, the excellent performances of rollers are required urgently [1-3]. The high speed steel (HSS) have been widely applied in roller manufacturing and made a breakthrough because of its good service performances [4-5].

At present, researches on HSS focus on molding techniques [6-7], the effects of alloy elements [8-9] and carbides on the roller performance, as well as the crack formation in HSS rollers [10]. However, the comprehensive properties of HSS, such as hardness, wear resistance, and red hardness, are closely related with the tempering process. After the tempering treatment, martensite decomposes and carbides precipitate, accompanying by the transformation of retained austenite in HSS. Meanwhile, the secondary hardening phenomenon appears [11]. Therefore, it is significant to investigate the behavior of morphology, distribution, and precipitation of carbides in HSS during the tempering process. HSS for roller contains many alloy elements, such as W, Mo, Cr, and V, which can form carbides as MC, $M_2C$, $M_6C$, $M_7C_3$, $M_{23}C_6$, and $M_3C$. The types of precipitated carbides can be decided by the composition of HSS. For a powder metallurgical HSS, ASP 23, tiny MC and $M_2C$ distribute in the matrix uniformly after tempering, and other carbides are not found [12]. However, the carbides precipitate unsimultaneously during the tempering process. Yamasaki [13] indicated that meta-stable carbides precipitated first, and then other stable carbides formed, accompanying by the dissolution of existing meta-stable carbides. Stable carbides can remain and meta-stable carbides change with temperature. Therefore, stable carbides make a great effect on the secondary hardening directly, while meta-stable carbides affect on that negatively, and finally influence the roll performance.

At present, few researches were made about stable and meta-stable carbides precipitated during the tempering process and it was difficult to distinguish from each other by experiment. Therefore, Thermo-Calc software,

Corresponding author: Qing-xiang Yang E-mail: qxyang@ysu.edu.cn

which can calculate alloy phase diagrams, was used. Meta-stable phase might appear after removing one or some existing phases from the equilibrium isopleths by Thermo-Calc, which was an effective method for analyzing the meta-stable equilibrium [13]. Therefore, different kinds of carbides precipitated in HSS during the tempering process were determined and predicted in this work, and stable and meta-stable carbides were also distinguished from each other.

## 2. Experimental

### 2.1. Materials

The experimental material was taken from a new HSS used for rollers, which was manufactured by centrifugal casting technology. The chemical composition of HSS for rollers is listed in Table 1.

**Table 1. Chemical composition of HSS** **wt%**

| C | Cr | Mo | V | W | Si | Nb | Mn | Fe |
|---|---|---|---|---|---|---|---|---|
| 1.4-1.5 | 4-5 | 4.5-5.0 | 3-4 | 4-5 | 1-1.5 | 0.6-1.0 | 0.8-1 | Bal. |

### 2.2. Method

Specimens with the dimension of 13 mm × 9 mm × 9 mm were first put into a crucible with the surfaces coated by the anti-oxidization coating Mp120, heated up to 1000°C at 20°C/min and 1360°C at 12°C/min, held for 5 min, and then quenched quickly into water after cooled to 1150°C in the furnace, finally tempered at 520°C after quenching. The phase structures of HSS for rollers were determined by a D/max-2500/PC X-ray diffractometer (XRD). The hardness of the specimens was measured by HR-150A Rockwell hardness test. The volume fraction of carbides was counted by Image-Pro Plus software. The typical microstructures were observed by an S4800-II field emission scanning electron microscope (FESEM) with energy disperse spectroscopy (EDS).

### 2.3. Calculation method

The Fe-C isopleths and the relationship between mass fraction and temperature of all phases at 1150°C were calculated by Thermo-Calc according to the chemical composition of HSS for rollers.

## 3. Results and discussion

### 3.1. XRD analysis of HSS after quenching and tempering

Figs. 1(a) and (b) are X-ray diffraction patterns of HSS for rollers after quenching at 1150°C and then tempering at 520°C. In Fig. 1, the peak of martensite decreases after tempering, because the martensite decomposes into tempered martensite and carbides. MC and $M_6C$ increase due to their precipitation from the matrix. In the position of $2\theta = 38.7°$, the peak of $M_2C$ increases. Meanwhile, the small peaks of $M_7C_3$ and $M_3C$ appear. Compared with the quenching process, it is known that the carbides MC, $M_2C$, $M_6C$, $M_3C$, and $M_7C_3$ in HSS precipitate from the matrix after the tempering process.

### 3.2. Hardness study of HSS after quenching and tempering

Table 2 lists the volume fraction of carbides and the hardness of the matrix after quenching at 1150°C and then tempering at 520°C. From Table 2, the volume fraction of carbides quenched at 1150°C is 7.466%, which reaches 8.462% after tempering at 520°C. The reason is that a large quantity of secondary carbides precipitate from the matrix and distribute dispersedly after tempering, resulting in the increase in volume fraction of carbides. Because of these small secondary carbides precipitated from the matrix and the "secondary quenching" of residual austenite after tempering, the secondary hardening appears and the hardness increases from HRC 56.5 after quenching at 1150°C to HRC 58.2 after tempering at 520°C.

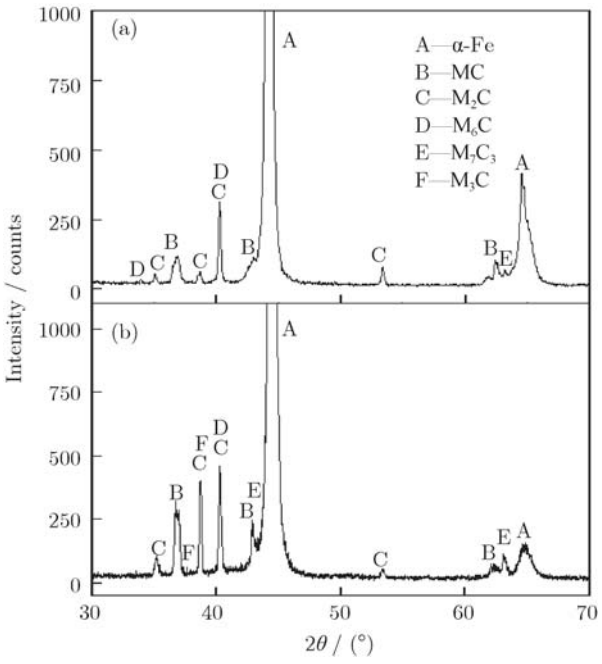


**Fig. 1. XRD patterns of carbides in HSS after quenching at 1150°C (a) and then tempering at 520°C (b).**

### 3.3. FESEM observation of HSS after tempering

The typical morphologies and EDS patterns of car-

**Table 2. Volume fraction of carbides and hardness of the matrix**

| Heat treatment | Volume fraction of carbides / % | Matrix hardness, HRC |
|---|---|---|
| 1150°C quenching | 7.466 | 56.5 |
| 1150°C quenching + 520°C tempering | 8.462 | 58.2 |

bides in HSS, quenching at 1150°C and tempering at 520°C, were observed and analyzed by FESEM with EDS.

From Fig. 2(a), the precipitated MC carbide is bulk-like in shape. The V content of this carbide is high accompanied by a certain amount of Nb. The atomic ratio of C to other elements is ∼1:1 from the EDS spectrum in Fig. 2(b). Serna and Rossi [14] investigated carbides in AISI M2 high speed steel and found the bulk-like MC carbides enriched with V element. From Fig. 3(a), the morphology of $M_2C$ carbide is a long stripe-like shape. The mass fraction of Mo reaches 38.49% and the contents of Cr, V, and W are relatively high according to the EDS result in Fig. 3(b). The $M_6C$ carbide in Fig. 4(a) has a special fishbone-like morphology and the high contents of Mo and Fe according to the EDS spectrum in Fig. 4(b). Yang *et al.* [15] once reported that $M_6C$ had a face center cubic (FCC) crystal structure with a lattice parameter $a = 110$ nm, which was rich in W or Mo and contained Fe and Cr. From Fig. 5, the $M_7C_3$ carbide with a daisy-like shape contains a certain amount of Cr and Mo. Refs. [16] and [17] point out that $M_7C_3$ is a Cr-rich carbide, and Fe and Mo are also soluble in this carbide.

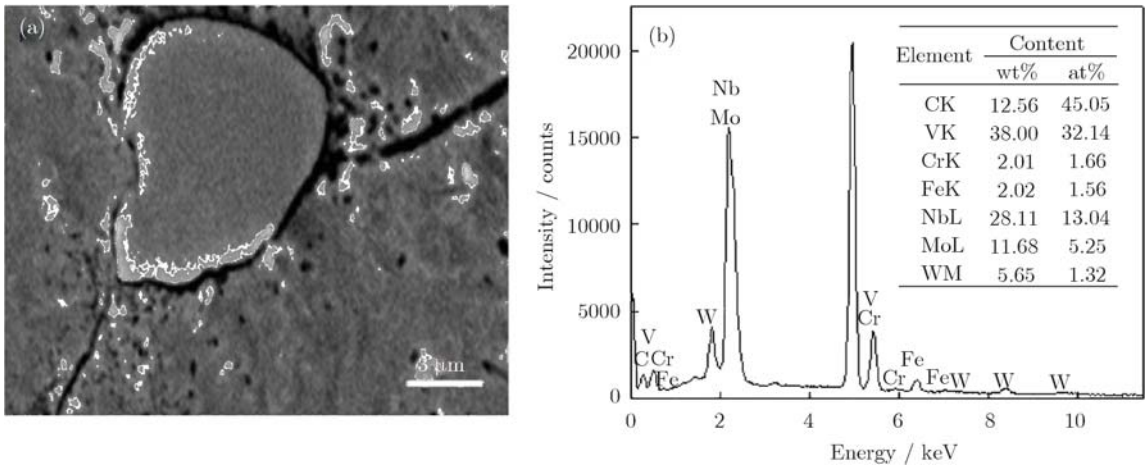


**Fig. 2. Typical morphology (a) and EDS spectrum (b) of bulk-like MC.**

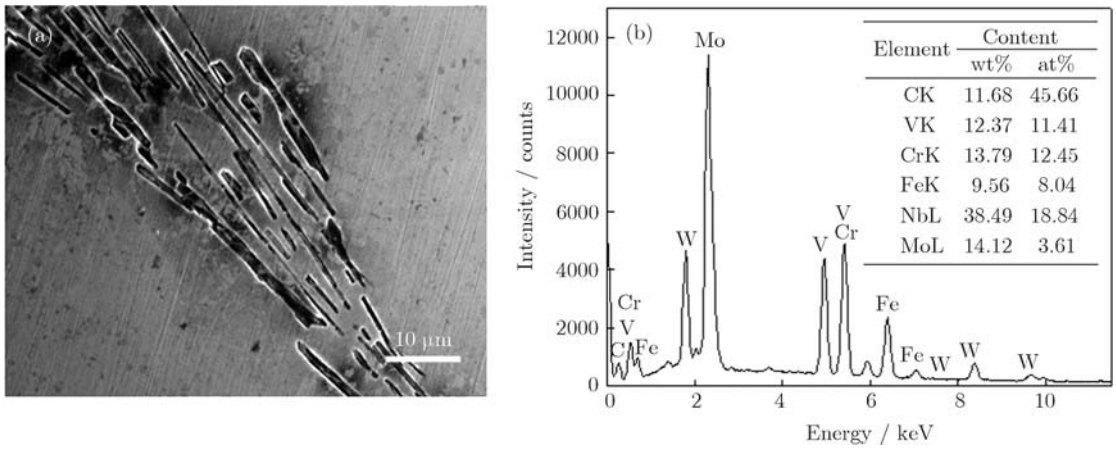


**Fig. 3. Typical morphology (a) and EDS pattern (b) of stripe-like $M_2C$.**

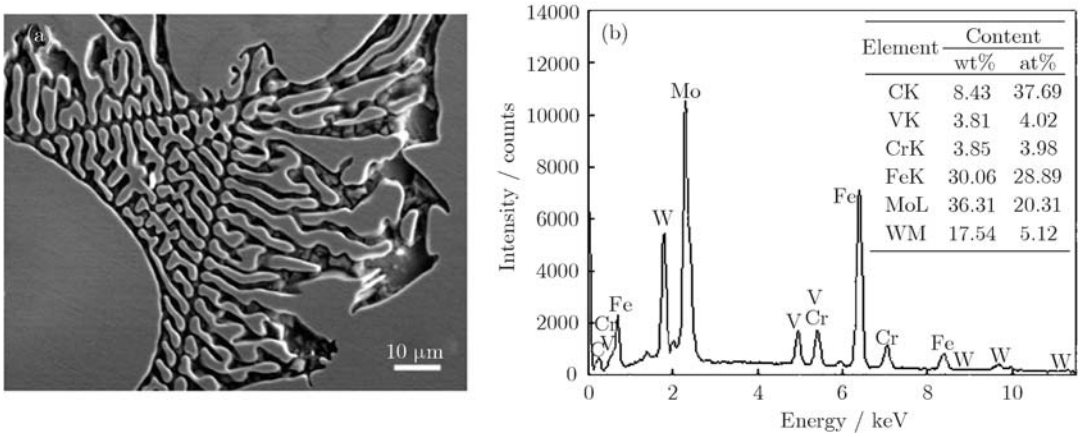


**Fig. 4. Typical morphology (a) and EDS pattern (b) of fishbone-like $M_6C$.**

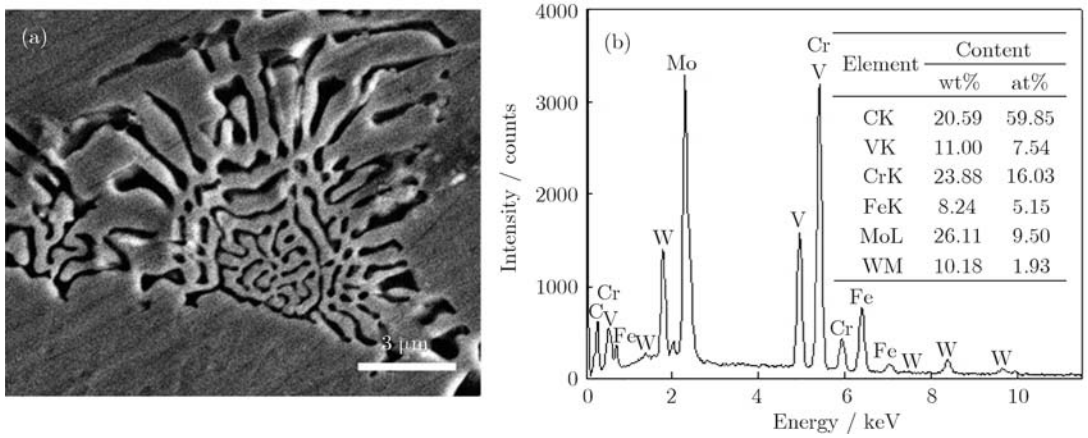


**Fig. 5. Typical morphology (a) and EDS pattern (b) of daisy-like $M_7C_3$.**

### 3.4. Analysis of stable and meta-stable carbides in HSS during tempering

The Fe-C isopleths of HSS calculated by Thermo-Calc are shown in Fig. 6. From Fig. 6, it is known that ferrite (α) + MC + $M_6C$ + $M_{23}C_6$ exists in HSS when it is cooled to room temperature at the equilibrium state. It is also seen that the equilibrium phases at 1150°C are austenite (γ) + MC + $M_6C$ in HSS. It is therefore considered that if the specimen is quenched at 1150°C, the high temperature microstructure can be retained, and γ phase transforms into martensite. The microstructure at room temperature can be martensite + MC + $M_6C$. However, $M_{23}C_6$, only existing at the equilibrium state, cannot be precipitated during the quenching process.

Fig. 7 shows the relationship between mass fraction and temperature of carbides during the tempering process. If the specimens are cooled at the equilibrium state according to Fig. 6, the equilibrium phases will be α + MC + $M_6C$ + $M_{23}C_6$. It is shown in Fig. 7(a), MC increases slightly, $M_6C$ reduces, and $M_{23}C_6$ changes unobviously. However, the microstructure at room temperature is martensite + MC + $M_6C$ without the precipitation of $M_{23}C_6$ after quenching at

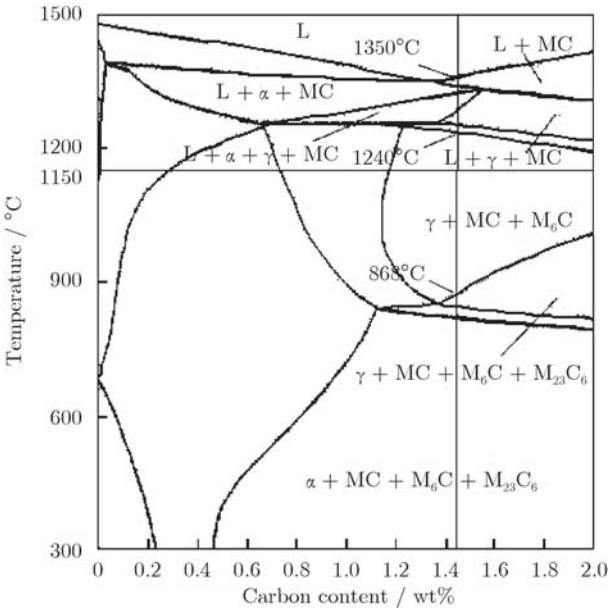


**Fig. 6. Fe-C isopleths of HSS for rollers.**

1150°C. From Fig. 7(b), after removing $M_{23}C_6$, $M_7C_3$ appears as a meta-stable carbide during the tempering process, and its mass fraction increases a little with the increase of temperature, and meanwhile, MC increases and $M_6C$ decreases slightly. By removing $M_{23}C_6$ and $M_7C_3$ in HSS, the curves of mass fraction vs. temperature of carbides are calculated as shown in Fig. 7(c). $M_2C$ and $M_3C$ appear. As a kind of meta-stable carbide, the nucleation of $M_3C$ is easier. As the time goes on, $M_3C$ dissolves accompanied by the nucleation of more stable carbides at the same place [13]. Therefore, $M_3C$ disappears in the phase diagram before 450°C. Therefore, $M_3C$ cannot be observed from the microstructure after tempering at 520°C and only a small peak is found in XRD patterns. MC changes unobviously, $M_2C$ increases sharply, and $M_6C$ decreases. The mass fraction of $M_2C$ is the largest, followed by $M_6C$, and then MC, which is in good agreement with the XRD result in Fig. 1(b) except $M_7C_3$ and $M_3C$. Combining the calculated results of Figs. 3 and 4, the stable phases are MC and $M_6C$, but the meta-stable ones are $M_2C$, $M_7C_3$, and $M_3C$ in HSS for rollers during the tempering process.

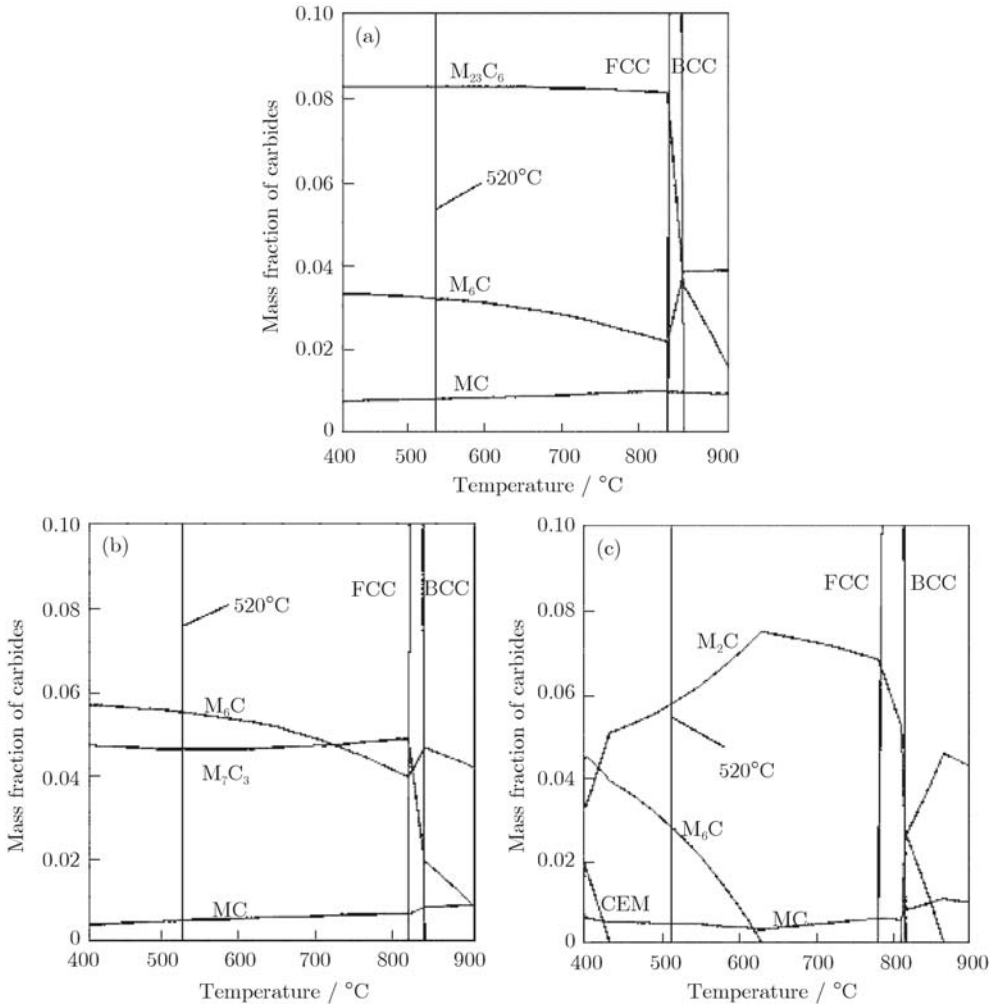


**Fig. 7. Relationship between mass fraction of carbides and temperature in a new HSS for rollers: (a) stable phases; (b) the phases after removing $M_{23}C_6$; (c) phases after removing $M_{23}C_6$ and $M_7C_3$.**

## 4. Conclusions

(1) Carbides MC, $M_2C$, $M_6C$, $M_7C_3$, and $M_3C$ exist in HSS for rollers during the tempering process according to XRD results.

(2) The hardness increases from HRC 56.5 to HRC 58.2, when the specimen is quenched at 1150°C and then tempered at 520°C.

(3) The precipitated phases in HSS for rollers are bulk-like MC, long stripe-like $M_2C$, fishbone-like $M_6C$, and daisy-like $M_7C_3$ during the tempering process.

(4) The Fe-C isopleths and the relationship between mass fraction and temperature of carbides at 1150°C cal-

culated by Thermo-Calc show that, the stable phases are MC and $M_6C$, and the meta-stable ones are $M_2C$, $M_7C_3$, and $M_3C$ in HSS for rollers during the tempering process. The calculated results are consistent with the experimental ones.

## Acknowledgements

The authors would like to express their gratitude for the project supported by the National Natural Science Foundation of China (No. 51271163).

### References

[1] C. Rodenburg and W.M. Rainforth, A quantitative analysis of the influence of carbides size distributions on wear behavior of high-speed steel in dry rolling/sliding contact, *Acta Mater.*, 55(2007), No. 7, p. 2443.

[2] J.W. Park, H.C. Lee, and S. Lee, Composition, microstructure, hardness, and wear properties of high speed steel rolls, *Metall. Mater. Trans. A*, 30(1999), No. 2, p. 399.

[3] H.G. Fu, Q. Xiao, and J.D. Xing, A study of segregation mechanism in centrifugal cast high speed steel rolls, *Mater. Sci. Eng. A*, 479(2008), No. 1-2, p 253.

[4] E.S. Lee, W.J. Park, K.H. Baik, and S. Ahn, Different carbide types and their effect on bend properties of a spray-formed high speed steel, *Scripta Mater.*, 39(1998), No. 8, p. 1133.

[5] C.K. Kim, J.I. Park, S. Lee, Y.C. Kim, N.J. Kim, and J.S. Yang, Effects of alloying elements on microstructure, hardness, and fracture toughness of centrifugally cast high-speed steel rolls, *Metall. Mater. Trans. A*, 36(2005), No. 1, p. 87.

[6] K.C. Hwang, S. Lee, and H.C. Lee, Effects of alloying elements on microstructure and fracture properties of cast high speed steel rolls: Part I. Microstructure analysis, *Mater. Sci. Eng., A*, 254(1998), No. 1-2, p. 282.

[7] K.C. Hwang, S. Lee, and H.C. Lee, Effects of alloying elements on microstructure and fracture properties of cast high speed steel rolls: Part II. Fracture behavior, *Mater. Sci. Eng., A*, 254(1998), No. 1-2, p. 296.

[8] S.Z. Wei, J.H. Zhu, L.J. Xu, and R. Long, Effects of carbon on microstructures and properties of high vanadium high-speed steel, *Mater. Des.*, 27(2006), No. 1, p. 58.

[9] S.Z. Wei, J.H. Zhu, and L.J. Xu, Effects of vanadium and carbon on microstructures and abrasive wear resistance of high speed steel, *Tribol. Int.*, 39(2006), No. 7, p. 641.

[10] H.W. Qu, B. Liao, L.G. Liu, D. Li, J. Guo, X.J. Ren, and Q.X. Yang, Precipitation rule of carbides in a new high speed steel for rollers, *Calphad*, 36(2012), p. 144.

[11] J.L. Liu and Q.Q. Luo, Tempering behaviour of hardened surface of T1 high speed tool steel after laser heating, *Mater. Lett.*, 16(1993), No. 2-3, p. 134.

[12] R. Wang and G.L. Dunlop, The crystallography of secondary carbide precipitation in high speed steel, *Acta Metall.*, 32(1984), No. 10, p. 1591.

[13] S. Yamasaki, *Modeling Precipitation of Carbides in Martensitic Steels* [Dissertation], Cambridge University, London, 2004, p. 52.

[14] M.M. Serna and J.L. Rossi, MC complex carbide in AISI M2 high-speed steel, *Mater. Lett.*, 63(2009), No. 8, p. 691.

[15] F.M. Yang, X.F. Sun, W. Zhang, Y.P. Kang, H.R. Guan, and Z.Q. Hu, Secondary $M_6C$ precipitation in K40S cobalt-base alloy, *Mater. Lett.*, 49(2001), No. 3-4, p. 160.

[16] H.G. Fu and J.D. Xing, *Manufacturing Technology of HSS Rollers*, Metallurgical Industry Press, Beijing, 2007, p. 73

[17] Y.K. Deng, J.R. Chen, and S.Z. Wang, *High Speed Tool Steels*, Metallurgical Industry Press, Beijing, 2002, p. 77.